TMEM16A Inhibits Autophagy and Promotes the Invasion of Hypopharyngeal Squamous Cell Carcinoma Through mTOR Pathway

Xin Yang
Yuhuangding Hospital
Limei Cui
Yuhuangding Hospital
Zhonglu Liu
Yuhuangding Hospital
Yumei Li
Yuhuangding Hospital
Xinxin Wu
Yuhuangding Hospital
Ruxian Tian
Yuhuangding Hospital
Chuanliang Jia
Yuhuangding Hospital
chao Ren
Shandong Provincial Innovation and Practice Base for Postdoctors, Yantai Yuhuangding Hospital
Yakui Mou
Yuhuangding Hospital
Xincheng Song
drxchsong@163.com

Qingdao University

Research Article

Keywords: hypopharyngeal squamous cell carcinoma, autophagy, TMEM16A, mTOR

Posted Date: March 14th, 2022

DOI: https://doi.org/10.21203/rs.3.rs-1430726/v1

Additional Declarations: No competing interests reported.

Version of Record: A version of this preprint was published at Carcinogenesis on March 12th, 2024. See the published version at https://doi.org/10.1093/carcin/bgae020.

Abstract

Background

Previous investigations indicated that transmembrane protein 16A (TMEM16A) mediates the pathogenesis and malignant of many tumors through regulating multiple pathways. However, whether TMEM16A could regulate autophagy via mammalian target of rapamycin (mTOR) pathway to modulate **hypopharyngeal squamous cell carcinoma** (HSCC) occurrence and development or not is still unclear.

Methods

The expression of TMEM16A in HSCC and metastatic lymph nodes was detected by immunohistochemistry and western blot. TMEM16A was overexpressed or knocked down in FaDu cell line to evaluate its effects on the biological function by cell colony formation experiment, wound healing assay, trans well assay, and invasion assay. TMEM16A was knocked down or over expression in FaDu cells to test apoptosis and autophagy related protein and autophagosome formation by western blot, transmission electron microscopy and immunofluorescence.

Results

In the present study, we observe that the expression level of TMEM16A in HSCC and metastatic lymph nodes are significantly higher than that in normal tissues. The results of in-vitro experiments showed that silencing TMEM16A significantly inhibited the proliferation, invasion and migration of HSCC cells. Silencing TMEM16A inhibited tumor formation in xenografted mice. Further experiments demonstrated that knocking down TMEM16A in HSCC cells could block the activation of mTOR, and thus promote the initiation of the autophagic death by activating sequestosome-1 (SQSTM1/P62) and protein light chain 3II (LC3II).

Conclusion

Therefore, TMEM16A displays an important effect on autophagy in HSCC, which may provide a potential therapeutic target for the treatment of HSCC.

Introduction

Hypopharyngeal squamous cell carcinoma (HSCC), which originates from submucosa, is the worst malignant tumor with the worst prognosis among the squamous cell carcinoma of the head and neck[1]. Because of its heterogeneity and complex anatomical structure, the disease has the characteristics of concealed location, easy infiltration and spread along the mucosa, and high rate of cervical lymph node metastasis. At the time of diagnosis, about 70–85% of the patient had evolved to stage III or IV, while the

overall 5-year survival rate of HSCC patients with III or IV is only 15–45% [2]. Despite advances in chemotherapy, radiation, and reconstructive surgery options, the 5-year survival rate of HSCC was not significantly improved [3]. The main factors affecting the prognosis of HSCC are recurrence and cervical lymph node metastasis [4, 5]. As a consequence, it is an unmet need to study the molecular mechanism of the initiation and progression of hypopharyngeal carcinoma, and to find new molecular biomarkers as predictors and therapeutic targets for patients with HSCC.

As we know, autophagy is a highly conserved cellular process in which cytoplasmic materials are degraded and recycled to maintain energy homeostasis. Accumulating evidence indicates that autophagy plays a vital role in maintaining homeostasis in cells. Autophagy is also closely related to the development of many diseases, especially in cancers [6]. The mTOR signaling is hyperactive in up to 80% of human cancers, in which context it plays a pivotal role in sustaining cancer cell growth and survival [7]. The studies indicate that a potent and persistent activation of autophagy via inhibition of the mTOR pathway, even in cancer cells where autophagy is occurring, can trigger premature senescence, cellular proliferation arrest [8].

TMEM16A (also known as anoctamin 1, ANO1) was identified as a Ca^{2+}- activated chloride channel in 2008[9, 10]. Abnormally high expression of TMEM16A was reported to promote cancer process and poor prognosis in colorectal cancer[11], esophageal squamous cell carcinoma [12], gastric cancer [13] and so on. Moreover, TMEM16A has been reported to play a role in malignant tumors through multiple pathways[14]. TMEM16A can activate Epidermal growth factor receptor (EGFR) and calmodulin dependent protein kinase II (CAMKII) signaling in breast cancer cells [15], mitogen-activated protein kinases (MAPK) signaling in SMMC-7721 cells [16]. Additionally, the role and molecular mechanism of TMEM16A regulating autophagy in malignant tumors, especially in HSCC, have not been discussed.

In this study, we detected the ectopic expression of TMEM16A in HSCC tumors and their metastatic lymph nodes, and explored the mechanism of TMEM16A acting on autophagy through mTOR *in vitro* HSCC FaDu cell line. Moreover, we found that knocking down TMEM16A can obviously impair cancer growth and invasion. All these results indicate TMEM16A plays an important role in HSCC progression, which enables TMEM16A to be a potential biomarker and target for the comprehensive treatment of hypopharyngeal carcinoma.

Materials And Methods

Tissue specimens of patients

All experiments were carried out after obtaining approval from Ethics Committee of Yantai Yuhuangding Hospital affiliated to Qingdao University, and all experiments were performed in accordance with guidelines set out by that institution. Before obtaining primary tissue samples, informed consent was obtained from each subject. From January 2016 to October 2020, 57 paraffin-embedded tissue specimens were collected from the Department of Pathology, Yantai Yuhuangding Hospital affiliated to

Qingdao University, including 57 cases of hypopharyngeal carcinoma, 57 cases of normal margin and 40 cases of lymph nodes. All patients with hypopharyngeal carcinoma did not receive radiotherapy or chemotherapy before operation. The surgical staging was determined according to the staging system. Two independent pathologists experienced in evaluating immunohistochemical (IHC) staining confirmed the results of all tissue sections. At the same time, the corresponding frozen tissue specimens were collected from 40 frozen tissue specimens archived in the Department of Otorhinolaryngology, head and neck surgery, Yantai Yuhuangding Hospital affiliated to Qingdao University, including 40 cases of hypopharyngeal carcinoma, 40 cases of normal margin and 40 cases of lymph nodes.

Cell Line Cultures

Human pharyngeal squamous cell carcinoma cell line FaDu (RRID: CVCL_1218), AMC-HN-9 (RRID: CVCL_5967), TU212 (RRID: CVCL_4915), 5-8F (RRID: CVCL_C528) and NP69SV40T (RRID: CVCL_F755) was purchased from cell bank of Chinese Academy of Sciences (shanghai, China). All cells were grown under standard cell culture conditions of 37°C 5% CO_2 and 95% humidity. The FaDu and NP69SV40T cells were cultured in Dulbecco's modified Eagle medium (DMEM, Gibco) with 10% fetal bovine serum (FBS, Gibco, USA), 100 IU/ml penicillin and 100μg/ml streptomycin and maintained at low passage number. AMC-HN-9 and 5-8F cells were cultured in 1640 (Gibco, USA). TU212 was cultured in DMEM/F12 (Gibco, USA). All cells were tested for mycoplasma contamination before use. All cell lines were genotyped to establish identity within 6 months of experimentation. Rapamycin was purchased from (Absin, shanghai), A 20 mM solution was prepared in dimethyl sulfoxide and stored at -20℃ for in vitro experiments.

Immunohistochemistry

Formalin-fixed and paraffin-embedded sections of hypopharyngeal carcinoma 57 tissues were used for immunohistochemistry.4-μm-thick paraffin blocks were incubated with anti-TMEM16A antibodies (1:100, Abcam, ab64085) at 1:100 overnight at 4 ℃. After rewarming and incubating with the secondary antibody (1:400, Absin, abs20002) for 30 min, signals were visualized using diaminobenzidine. Finally, the expression of TMEM16A was evaluated according to the area and expression intensity. The intensity of immunoreactivity was scored as follows: 0 for no staining, 1 for weak staining, 2 for moderate staining, and 3 for strong staining. The IHC score was determined by the multiplication of the intensity score (0–3) and the percentage (0-100%) of immunopositive cells, resulting in the final IHC score ranging from 0 to 300.

Western blot

For analysis in western blots equal amounts of protein were denatured, separated in 12% acrylamide gels and transferred to nitrocellulose membrane. Nitrocellulose membranes were incubated with anti-TMEM16A antibodies (1:1000, Abcam, ab64085), anti-mTOR polyclonal antibody (1:1000, CST,2983T), anti-LC3 polyclonal antibody (1:1000, CST,12741T), anti-P62 polyclonal antibody (1:1000, CST, 8025T) and anti-Actin antibody (1:1000, CST, 3700T), respectively, at a dilution of 1:1000 overnight at 4°C. After washing 3 times with TBST, the blots were exposed to the goat secondary antibody conjugated to

horseradish peroxidase at a dilution of 1:5000 (Absin, China) at room temperature and visualized using an enhanced chemiluminescent (ECL) kit (Beyotime, China) on a ChemiDocMP imaging System (BIO-RAD, China).

Wound Healing Assay

The cells were plated in DMEM plus 10% Fetal Bovine Serum in a 6-well culture plate and grown to confluence. Once confluent, a wound was scraped with a sterile 1ml tip, and washed twice with PBS. Cells were photographed at 0, 24, 48, or 72h under an inverted microscope (Nikon) at 40× magnification. The wound healing area we calculated using the ImageJ software (National Institutes of Health, Bethesda, Maryland), and the relative scratch area was determined by the ratio of the average area in the treated cells to that in the control cells.

Migration assay and Invasion assay

Experiments were carried out in Transwell 24-insert plate chambers (Corning, NY, USA). The cell migration experiment was performed by seeding 5×10^4 shTMEM16A and ANO1 LV cells in 100 μL of medium with 1% FBS (Gibco-Invitrogen, Carlsbad, CA, USA) into the upper compartment of the chamber with a polycarbonate filter (6.5-mm diameter, 8-mm pores; Corning Costar, Corning, NY, USA). The lower chambers contained 600uL of medium containing 10% FBS (Gibco) to serve as chemoattractant. For the cell invasion experiment, Transwells were coated-with Matrigel (BD Biosciences, Franklin Lakes, NJ, USA). The migrated or invaded cells in the lower surface of the filters were fixed with methanol, stained with Giemsa (Coolaber, Beijing, China) and counted under a light microscope (Olympus Corp, Tokyo, Japan) in 5 randomly selected visual fields at magnification of 400×.

Tumor xenograft model and analysis

Animal facilities and experiments were in accordance with local institutional guidelines and approved by the local animal welfare committee. BALB/c athymic nude mice (female, 4–6 weeks old, weighing 16–20 g) were bred in pathogen-free conditions at 25°C with 12 h light/dark cycle. Animals received water and food ad libitum. Mice were randomly divided into two groups of shTMEM16A and control with 3 animals in each group. Equal numbers (1.5×10^6) of shTMEM16A or shTMEM16A-Scrambled cells in 200ul PBS were implanted subcutaneously into mouse right flank. The subsequent tumor volumes were measured when a palpable tumor was noticed. Tumor sizes were recorded every week and the volume was calculated. The end point of the experiment was set on the 28th day after implantation of FaDu cells. Mice were euthanized before tumors were removed for weighing. The tumor volume was calculated using the after formula: Tumor volume (in mm^3) = (a × b2)/2, a represents the length and b represents the width. Lysates of tumors were prepared and protein was estimated.

Transmission Electron microscopy

Cells were fixed in 2.5% glutaraldehyde in 0.1 M sodium cacodylate for 45 minutes, washed and post fixed with 1% OsO4 for 30 minutes. The cells were again washed and stained for 5 minutes in 2.5% aqueous uranyl acetate. The samples were dehydrated with graded alcohol and embedded on Epon resin

(Canemco Inc). Ultrathin sections were cut on a Leica EM microtome, counterstained with 5% uranyl acetate and 0.3% lead citrate and observed under electron microscope.

Immunofluorescence

Fadu cells were cultured normally for 12 h before the experiment. Cells were incubated in 4% paraformaldehyde (Solarbio, Beijing, China) for 20 min. Cells were washed with PBS and permeabilized with 0.5% Triton X-100 in PBS for 20 min. Next, nonspecific protein binding sites were blocked with 5%BSA for 2h. Cells were incubated with the following antibodies diluted in PBS with 3%BSA overnight at 4°C: anti-LC3 (1:1000, 3638T, CST, USA). After washing with PBS, cells were further incubated for 1h at 37°C with an anti-rabbit secondary antibody (AF594; Jackson). Samples were next stained with Hoechst 33342 (Aladdin Biochemical Technology Co., Ltd., Shanghai, China) for 10 min. Images were recorded using a fluorescence microscope (Olympus, Tokyo, Japan). In 5 randomly selected visual fields at magnification of 400×.

Colony formation assays

7.5×10^2 cells were plated in DMEM plus 10% Fetal Bovine Serum in 6-well plates and allowed to attach overnight. After 14 days incubation at 37℃ in an atmosphere containing 5% CO_2. Plates were fixed and stained with 0.05% crystal violet. Colonies were counted and data was normalized to the untreated control. Details of cell lines, and incubation times are included in figure captions.

Lentivirus transfection

Human TMEM16A (GenBank NM_018043) cloned into GV492 vector was used for overexpression in cells. For TMEM16A knockdown, scrambled short-hairpin RNA (TTCTCCGAACGTGTCACGT) and shRNA (CATCGGAATCTGGTACAATAT) were purchased from GENECHEM (Shanghai, China). TMEM16A expression levels from knockdown and expression samples were assessed by western blot.

Statistics

All data were presented as the mean ± SD. Statistical analysis was performed using student's t-test to compare two groups. The significance of statistical analysis was clarified by *P < 0.05 and **P < 0.01.

Results

1. The expression of TMEM16A in HSCC was higher than that in normal tissues.

We selected 57 patients with HSCC which were diagnosed as primary disease, without systemic disease and treatment. The results of IHC staining confirmed that the expression of TMEM16A in HSCC was higher than that in normal tissues (Fig. 1A,1B and 1E). The expression of TMEM16A in lymph gland was higher in HSCC patients with lymphatic metastasis than that in those without lymphatic metastasis (Fig. 1B and 1C).

In addition, we also carried out Western blot and found that the expression of TMEM16A was consistent with that of IHC (Fig. 1D and 1F).

2. Overexpression and down-regulation of TMEM16A affect cell growth, migration and invasion.

According to our previous detection results of TMEM16A in HSCC, we consider its role in the progression of HSCC. We used western blot to detect the expression of TMEM16A in laryngeal carcinoma cell lines AMC-HN-9, TU212, pharynx carcinoma cell line FaDu and 5-8F. We used the human nasopharyngeal epithelial cell line (NP69) as the normal control. The final results showed that the expression of FaDu was the highest, followed by TU212, and the expression of NP69 was the lowest. Therefore, we used FaDu cell line to carry out related functional experiments *in vitro*. We constructed FaDu cells with TMEM16A silencing and TMEM16A overexpression (OE) by transfecting TMEM16A shRNA lentivirus and TMEM16A OE lentivirus, respectively. The successful construction of the cell line was verified by Western blot (Fig. 2A).

Then, we used colony formation to analyze cell proliferation. Wound healing migration test, transport cell migration test and invasion test were used to evaluate the migration and invasion ability of FaDu cells in the control group. Clone formation analysis showed that the clone formation rate of FaDu cells TMEM16A OE was significantly higher than that of control cells (181.7 ± 11.02 vs. 110.7 ± 3.48, $P < 0.01$, Fig. 2B). The clone formation rate of shTMEM16A cells was significantly lower than that of untreated cells (113 ± 9.574 vs. 265 ± 6.608, $P < 0.01$, Fig. 3B). The migration experiment of wound healing showed that compared with the control group, the cells overexpressed by TMEM16A showed stronger migration ability and faster narrowed healing boundary (Fig. 2C, $P < 0.01$). This phenomenon was significantly reversed by shTMEM16A(Fig. 2C). Both the number of migrated cells in the Transwell experiment and the number of invasive cells were determined by counting the cells on the lower side of the filter. The results showed that the numbers of migration (93 ± 9.849 vs 263 ± 9.574, $P < 0.01$, Fig. 2D) and invasion (87 ± 13.3 vs 258.8 ± 15.72, $P < 0.01$, Fig. 2D) of FaDu cells overexpressed by TMEM16A were significantly higher than those in the control group. Compared with shTMEM16A cells, the number of migrating cells (271 ± 9.983 vs. 69.5 ± 12.74, $P < 0.01$, Fig. 3D) and invasive cells (275 ± 18.79 vs. 69 ± 13.3, $P < 0.01$, Fig. 3D) in shTMEM16A group decreased significantly. To sum up, the *in vitro* experimental results show that the high expression of TMEM16A can promote the proliferation of FaDu cells and enhance the ability of migration and invasion of FaDu cells. Silencing TMEM16A inhibits the proliferation, migration and invasion of FaDu cells.

3. Down-regulation of TMEM16A inhibits tumorigenicity in mice.

In order to verify the role of TMEM16A in tumorigenesis and growth *in vivo*, FaDu cells transfected with shTMEM16A lentivirus were subcutaneously injected into nude mice. At the same time, the cells transfected with control lentivirus were injected as control experiments. Mice were randomly divided into two groups and injected with shTMEM16A and control lentivirus respectively. The tumor tissue began to form on the 6th day after injection. On the 14th day after injection, the tumor in the control group showed irregular swelling, borderline and keratinization, while the tumor in the shTMEM16A group grew slowly

(Fig. 3A). The tumor growth curve of the control group showed that the tumor grew rapidly, and there was a significant difference in tumor growth between the experimental group and the control group on the 14th day of injection (Fig. 3B, $P < 0.01$). The measurement of tumor weight showed that the tumor weight of mice injected with shTMEM16A cells was significantly lower than that of control mice (Fig. 3C, $P < 0.01$). The tumor tissues were collected and further analyzed by Western blot(Fig. 3D)and IHC(Fig. 3E). The results showed that the expression of TMEM16A in shTMEM16A group was significantly down-regulated. It is suggested that silencing TMEM16A can reduce the tumorigenicity of FaDu cells *in vivo*.

4. Down-regulation of TMEM16A induces autophagy to cause cell death in FaDu cell.

Autophagy is a widespread cellular pathway which is associated with tumor progression[17]. When we silenced TMEM16A, we found that FaDu cells did not show typical apoptotic morphological changes. In order to determine whether silent TMEM16A regulates autophagy, we detected autophagy markers p62, LC3-I and LC3-II to observe the occurrence of autophagy by western blot. The results showed that compared with the untreated cells, the expression of p62 was significantly decreased in the cells silenced by TMEM16A, while the expression of LC3-II/LC3-I was significantly decreased and the expression of p62 was increased in the cells with OE of TMEM16A (Fig. 4A). At the same time, autophagy vacuoles increased in the cells silenced by TMEM16A under electron microscope (Fig. 4B). In order to detect the distribution of LC3, we performed immunofluorescence staining and found that the staining spots of LC3 increased significantly in the cells with silenced TMEM16A, while decreased in the untreated cells (Fig. 4C). The accumulation of LC3-II suggests that the formation of upstream autophagosomes is increased or the downstream autophagy-lysosome fusion is impaired. In order to clearly verify the specific effect of knocking down TMEM16A on autophagy, we chose chloroquine, an autophagy inhibitor that can inhibit the fusion of autophagosomes and lysosomes. After the addition of chloroquine to TMEM16A silenced cells, the number of LC3 staining spots in FaDu cells was higher than that in TMEM16A silenced cells (Fig. 4C). This experimental result are consistent with those of western blot (Fig. 4A). These results provide evidence for the autophagy of FaDu cells induced by silenced TMEM16A.

Then, through western blot experiments, we found that the expression of apoptosis marker caspase-3 was significantly decreased (Fig. 4D), which means TMEM16A silence could not induce apoptosis. These indicated that cell death induced by silencing TMEM16A was through the activation of autophagy but not through apoptosis.

5. TMEM16A down-regulates autophagy of hypopharyngeal carcinoma FaDu cells through affecting mTOR pathway

In our experiments, we found that the expression of mTOR decreased when TMEM16A was silenced and increased when overexpressing TMEM16A. Then we added rapamycin to inhibit mTOR in FaDu cells with TMEM16A overexpression and found that the expression of mTOR decreased significantly, while the expression of LC3-II increased (Fig. 5A and.5B). Finally, we re-tested the colony formation test, wound healing test, migration and invasion test of the TMEM16A overexpressed FaDu cells added with rapamycin. The results showed that compared with the control group, the ability of colony formation was

decreased when adding rapamycin in TMEM16A overexpressed FaDu cells (figure.5E), the ability of wound healing slowed down (Fig. 5F), and the ability of migration and invasion were significantly inhibited (Fig. 5G). Therefore, it is suggested by *in vitro* experiments that silent TMEM16A inhibits the invasion and metastasis of FaDu cells through autophagy induced by mTOR.

Discussion

Because of its tendency for late presentation, HSCC often presents in an advanced stage and its prognosis is notoriously poor. It remains a challenge for head and neck oncologist to manage HSCC in diagnosis and treatment[18].The lack of diagnostic markers and new therapeutic targets for HSCC emphasized the need to rapidly improve understanding of the molecular mechanisms of HSCC invasion and metastasis.

In this study, we explored the role of TMEM16A in the invasion and metastasis of HSCC through *in vivo* and *in vitro* experiments. The results show that TMEM16A regulates the invasion and metastasis of HSCC through autophagy through mTOR. The most important thing is that we found that inhibition of TMEM16A through mTOR-regulated autophagy will inhibit the invasion and metastasis of HSCC, which also provides a new idea for the treatment of HSCC.

By examining the tumor tissue samples of patients with HSCC, we found that TMEM16A expression was significantly increased in HSCC tissues. Our present data are consistent with study by Dixit *et al.* [19]. Moreover, we found that TMEM16A was highly expressed both in HSCC and in metastatic lymph nodes, which was the same as that reported by Shiwarski *et al*.[20]. But we also found that the expression of TMEM16A in metastatic lymph nodes was higher than that in non-metastatic lymph nodes. At the same time, our results showed that there was no significant difference in the expression of TMEM16A between hypopharyngeal carcinoma and metastatic lymph nodes. But Shiwarski *et al*. reported that the expression of TMEM16A in metastatic lymph nodes of HNSCC patients was lower than that of primary lymph nodes[20]. The point of view here is different from that of us. The possible reason for this is that in this paper, we only select HSCC, which is the most malignant tumor of the head and neck, as the object of study.

Here, we demonstrated that TMEM16A gene knockdown can significantly inhibit proliferation, migration and invasion in FaDu cell lines. Preclinical trials testing shTMEM16A lentivirus showed a decrease in cell proliferation, decrease of tumor growth in mice xenografts. When TMEM16A is overexpressed, the state of FaDu cells is the opposite. This is consistent with most researchers. Some scholars have found that loss of TMEM16A can inhibit the proliferation in head and neck squamous cell carcinoma (HNSCC), but they did not mention about whether it affected the ability of migration and invasion in HNSCC[21]. Otherwise, some scholars also have shown that TMEM16A gene knockout can significantly inhibit the migration and invasion of gastric cancer cells, but does not affect its proliferation[22]. This shows that the biological behavior of TMEM16A is different in various tumors. Current studies on tumors have found that TMEM16A has multifaceted roles on a variety of molecular targets, which focus on a variety of

carcinogenic functions regulated by TMEM16A. Initially, Brit-schgi *et al.* report that TMEM16A expression is able to regulate EGFR constitutive phosphorylation and associated signaling pathways such as sport-related concussion (SRC), protein kinase B (Akt), Human Epidermal Growth Factor Receptor 2 (HER2), extracellular regulated protein kinases (ERK) and CAMK II in HNSCC and breast cancer cells[15, 23]. Some author found that TMEM16A is required for promoting EGF-induced EGFR signaling in a pancreatic cancer cell line[24].

However, whether TMEM16A affects the biological behavior of tumor through autophagy has not been studied. Autophagy is complex in cancer. Researchers have favored the view of a double-edged sword role of autophagy in tumors. On the one hand, numerous reports have demonstrated pro-tumorigenic roles of autophagy, the crucial role of autophagy in malignant cells and stromal cells in promoting tumor growth, primarily in cancers driven by kirsten rat sarcoma viral oncogene (KRAS) that require high cellular metabolic activity to sustain survival[17]. On the other hand, autophagy can suppress the process of tumor through suppressing tumor-promoting inflammatory signals and enhancing the anticancer immune function of myeloid cells in tumor microenvironment[25, 26].

Our study showed that when TMEM16A was knocked down, western blot showed that the expression of LC3II increased significantly and the expression of p62 decreased. Immunofluorescence showed that LC3II aggregation increased significantly, and a large number of autophagy lysosomes were observed in electron microscope. When chloroquine was added, western blot and immunofluorescence detection showed that the expression of LC3II increased. The above results show that knocking down TMEM16A promotes the production of autophagy. Interestingly, in the results of electron microscopy, we also observed that there was an abnormal increase in the morphology of mitochondria in the cells with autophagy, considering the possibility of mitochondrial autophagy at the same time.

We verified *in vitro* that TMEM16A could promote the proliferation, invasion and migration of HSCC FaDu cell line, while apoptosis marker caspase-3 decreased, LC3 II increased and p62 decreased.

Autophagy is regulated by mTOR (mammalian target of rapamycin)-dependent and mTOR-independent pathways [27, 28]. On one hand, mTOR can affect the activity of phosphatidylinositol-3-kinase (PI3K) complex by inhibiting ULK1, thus inhibiting autophagy. On the other hand, Beclin1 in the PI3K complex can be regulated by B-cell lymphoma-2 (Bcl-2) and bypass mTOR to directly regulate autophagy. mTOR as a serine kinase, its abnormal expansion can promote tumor proliferation, but the specific mechanism of mTOR to autophagy is not clear.

Some scholars have found that the effect of TMEM16A on autophagy does not depend on mTOR pathway [29], but is related to the decrease of kinase activity of vacuolar protein sorting 34 (Vps34) enzyme. This is different from our research. In this experiment, we knocked out TMEM16A and found that with the decrease of TMEM16A protein, the protein amount of mTOR also decreased. After the overexpression of TMEM16A, it was found that the expression of mTOR increased and autophagy was suppressed. At the same time, after the addition of mTOR inhibitor rapamycin, the expression of mTOR decreased significantly, while the expression of TMEM16A did not change significantly, and autophagy

increased. In this experiment, knocking out TMEM16A inhibits mTOR expression and promotes the autophagy production, indicating that TMEM16A may induce autophagy depending on mTOR inhibition.

Conclusions

To sum up, our study provides evidence that *in vitro* experiments, in hypopharyngeal carcinoma cell line FaDu, knockout TMEM16A positively regulates autophagy, negatively regulates apoptosis, and inhibits related tumor biological behavior. At the same time, it is verified that the regulation of autophagy by TMEM16A is realized by mTOR. These findings provide new insights into the mechanism that TMEM16A affects the invasion and metastasis of HSCC, and suggest a promising idea for targeted treatment of this disease.

Abbreviations

HSCC
hypopharyngeal squamous cell carcinoma
TMEM16A
also known as anoctamin 1, ANO1
EGFR
Epidermal growth factor receptor
MAPK
mitogen-activated protein kinases
CAMKII
calmodulin dependent protein kinase II
mTOR
mammalian target of rapamycin
HNSCC
head and neck squamous cell carcinoma
SRC
sport-related concussion
Akt
protein kinase B
HER2
Human Epidermal Growth Factor Receptor 2
ERK
extracellular regulated protein kinases
KRAS
kirsten rat sarcoma viral oncogene
LC3
protein light chain 3

SQSTM1/p62
sequestosome-1
PI3K
phosphatidylinositol-3-kinase
Bcl-2
B-cell lymphoma-2
Vps34
vacuolar protein sorting 34.

Declarations

Ethics approval and consent to participate

All experiments were carried out after obtaining approval from Ethics Committee of Yantai Yuhuangding Hospital affiliated to Qingdao University, and all experiments were performed in accordance with guidelines set out by that institution. Before obtaining primary tissue samples, informed consent was obtained from each subject. Animal facilities and experiments were in accordance with local institutional guidelines and approved by the local animal welfare committee.

Acknowledgment

not applicable

Consent for publication

All the co-authors consent to publish the work in Cell Communication & Signaling.

Availability of supporting data

The datasets generated during and/or analyzed during the current study are available from the corresponding author on reasonable request.

Competing interests

The authors declare that they have no competing interests.

Funding

This work was supported by the Natural Science Foundation of Shandong Province (grant number: ZR2019PH113), and Taishan Scholars Project (No.ts20190991).

Author contributions:

YKM and XCS conceived and designed the study. ZLL, XXW, RXT and CLJ collected human materials and data. XY and LMC performed the experiments. CR and YML analyzed and interpreted the data. XY wrote

the manuscript. All authors critically revised the manuscript.

References

1. Garneau JC, Bakst RL, Miles BA: **Hypopharyngeal cancer: A state of the art review.** *Oral Oncol* 2018, **86:**244-250.
2. Jang JY, Kim EH, Cho J, Jung JH, Oh D, Ahn YC, Son YI, Jeong HS: **Comparison of Oncological and Functional Outcomes between Initial Surgical versus Non-Surgical Treatments for Hypopharyngeal Cancer.** *Ann Surg Oncol* 2016, **23:**2054-2061.
3. Gatta G, Botta L, Sánchez MJ, Anderson LA, Pierannunzio D, Licitra L: **Prognoses and improvement for head and neck cancers diagnosed in Europe in early 2000s: The EUROCARE-5 population-based study.** *Eur J Cancer* 2015, **51:**2130-2143.
4. Chung EJ, Kim GW, Cho BK, Park HS, Rho YS: **Pattern of lymph node metastasis in hypopharyngeal squamous cell carcinoma and indications for level VI lymph node dissection.** *Head Neck* 2016, **38 Suppl 1:**E1969-1973.
5. Xing Y, Zhang J, Lin H, Gold KA, Sturgis EM, Garden AS, Lee JJ, William WN, Jr.: **Relation between the level of lymph node metastasis and survival in locally advanced head and neck squamous cell carcinoma.** *Cancer* 2016, **122:**534-545.
6. Sridhar S, Botbol Y, Macian F, Cuervo AM: **Autophagy and disease: always two sides to a problem.** *J Pathol* 2012, **226:**255-273.
7. Menon S, Manning BD: **Common corruption of the mTOR signaling network in human tumors.** *Oncogene* 2008, **27 Suppl 2:**S43-51.
8. Nam HY, Han MW, Chang HW, Kim SY, Kim SW: **Prolonged autophagy by MTOR inhibitor leads radioresistant cancer cells into senescence.** *Autophagy* 2013, **9:**1631-1632.
9. Yang YD, Cho H, Koo JY, Tak MH, Cho Y, Shim WS, Park SP, Lee J, Lee B, Kim BM, et al: **TMEM16A confers receptor-activated calcium-dependent chloride conductance.** *Nature* 2008, **455:**1210-1215.
10. Caputo A, Caci E, Ferrera L, Pedemonte N, Barsanti C, Sondo E, Pfeffer U, Ravazzolo R, Zegarra-Moran O, Galietta LJ: **TMEM16A, a membrane protein associated with calcium-dependent chloride channel activity.** *Science* 2008, **322:**590-594.
11. Mokutani Y, Uemura M, Munakata K, Okuzaki D, Haraguchi N, Takahashi H, Nishimura J, Hata T, Murata K, Takemasa I, et al: **Down-Regulation of microRNA-132 is Associated with Poor Prognosis of Colorectal Cancer.** *Ann Surg Oncol* 2016, **23:**599-608.
12. Shi ZZ, Shang L, Jiang YY, Hao JJ, Zhang Y, Zhang TT, Lin DC, Liu SG, Wang BS, Gong T, et al: **Consistent and differential genetic aberrations between esophageal dysplasia and squamous cell carcinoma detected by array comparative genomic hybridization.** *Clin Cancer Res* 2013, **19:**5867-5878.
13. Cao Q, Liu F, Ji K, Liu N, He Y, Zhang W, Wang L: **MicroRNA-381 inhibits the metastasis of gastric cancer by targeting TMEM16A expression.** *J Exp Clin Cancer Res* 2017, **36:**29.

14. Wang H, Zou L, Ma K, Yu J, Wu H, Wei M, Xiao Q: **Cell-specific mechanisms of TMEM16A Ca(2+)-activated chloride channel in cancer.** *Mol Cancer* 2017, **16:**152.
15. Britschgi A, Bill A, Brinkhaus H, Rothwell C, Clay I, Duss S, Rebhan M, Raman P, Guy CT, Wetzel K, et al: **Calcium-activated chloride channel ANO1 promotes breast cancer progression by activating EGFR and CAMK signaling.** *Proc Natl Acad Sci U S A* 2013, **110:**E1026-1034.
16. Deng L, Yang J, Chen H, Ma B, Pan K, Su C, Xu F, Zhang J: **Knockdown of TMEM16A suppressed MAPK and inhibited cell proliferation and migration in hepatocellular carcinoma.** *Onco Targets Ther* 2016, **9:**325-333.
17. Kimmelman AC, White E: **Autophagy and Tumor Metabolism.** *Cell Metab* 2017, **25:**1037-1043.
18. Kwon DI, Miles BA: **Hypopharyngeal carcinoma: Do you know your guidelines?** *Head Neck* 2019, **41:**569-576.
19. Dixit R, Kemp C, Kulich S, Seethala R, Chiosea S, Ling S, Ha PK, Duvvuri U: **TMEM16A/ANO1 is differentially expressed in HPV-negative versus HPV-positive head and neck squamous cell carcinoma through promoter methylation.** *Sci Rep* 2015, **5:**16657.
20. Shiwarski DJ, Shao C, Bill A, Kim J, Xiao D, Bertrand CA, Seethala RS, Sano D, Myers JN, Ha P, et al: **To "grow" or "go": TMEM16A expression as a switch between tumor growth and metastasis in SCCHN.** *Clin Cancer Res* 2014, **20:**4673-4688.
21. Duvvuri U, Shiwarski DJ, Xiao D, Bertrand C, Huang X, Edinger RS, Rock JR, Harfe BD, Henson BJ, Kunzelmann K, et al: **TMEM16A induces MAPK and contributes directly to tumorigenesis and cancer progression.** *Cancer Res* 2012, **72:**3270-3281.
22. Wanitchakool P, Wolf L, Koehl GE, Sirianant L, Schreiber R, Kulkarni S, Duvvuri U, Kunzelmann K: **Role of anoctamins in cancer and apoptosis.** *Philos Trans R Soc Lond B Biol Sci* 2014, **369:**20130096.
23. Fujimoto M, Kito H, Kajikuri J, Ohya S: **Transcriptional repression of human epidermal growth factor receptor 2 by ClC-3 Cl(-) /H(+) transporter inhibition in human breast cancer cells.** *Cancer Sci* 2018, **109:**2781-2791.
24. Crottès D, Lin YT, Peters CJ, Gilchrist JM, Wiita AP, Jan YN, Jan LY: **TMEM16A controls EGF-induced calcium signaling implicated in pancreatic cancer prognosis.** *Proc Natl Acad Sci U S A* 2019, **116:**13026-13035.
25. Grumati P, Morozzi G, Hölper S, Mari M, Harwardt MI, Yan R, Müller S, Reggiori F, Heilemann M, Dikic I: **Full length RTN3 regulates turnover of tubular endoplasmic reticulum via selective autophagy.** *Elife* 2017, **6**.
26. Ma Y, Galluzzi L, Zitvogel L, Kroemer G: **Autophagy and cellular immune responses.** *Immunity* 2013, **39:**211-227.
27. Kennedy BK, Lamming DW: **The Mechanistic Target of Rapamycin: The Grand ConducTOR of Metabolism and Aging.** *Cell Metab* 2016, **23:**990-1003.
28. Sarkar S: **Regulation of autophagy by mTOR-dependent and mTOR-independent pathways: autophagy dysfunction in neurodegenerative diseases and therapeutic application of autophagy enhancers.** *Biochem Soc Trans* 2013, **41:**1103-1130.

29. Lv XF, Zhang YJ, Liu X, Zheng HQ, Liu CZ, Zeng XL, Li XY, Lin XC, Lin CX, Ma MM, et al: **TMEM16A ameliorates vascular remodeling by suppressing autophagy via inhibiting Bcl-2-p62 complex formation.** *Theranostics* 2020, **10:**3980-3993.

Figures

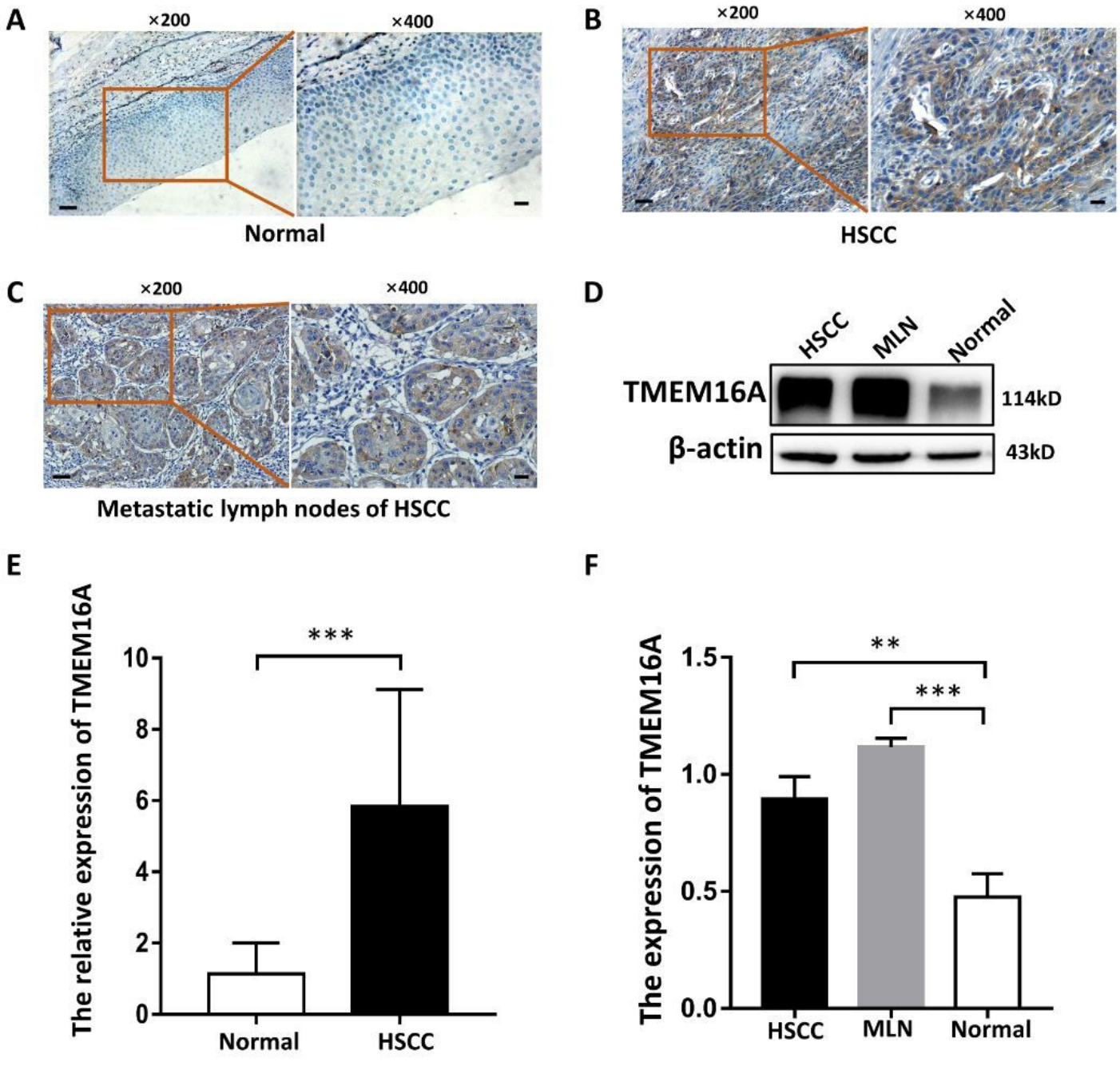

Figure 1

IHC was used to analyze the expression of TMEM16A in 57 pairs of HSCC and normal tissues.

A Immunohistochemistry was used to analyze the expression of TMEM16A in normal tissues. Scale bar:50um (left) or 20um(right). **B, C** Immunohistochemistry was used to analyze the expression of TMEM16A in HSCC and metastatic lymph nodes. Scale bar:50um (left) or 20um(right). **D** Representative result of detecting the expression of TMEM16A in HSCC, MLN and normal tissues by western blot. **E** The results of statistical analysis of 57 pairs of HSCC and normal tissues. **F** Expression of TMEM16A as measured by western blot in HSCC, MLN and normal tissues.

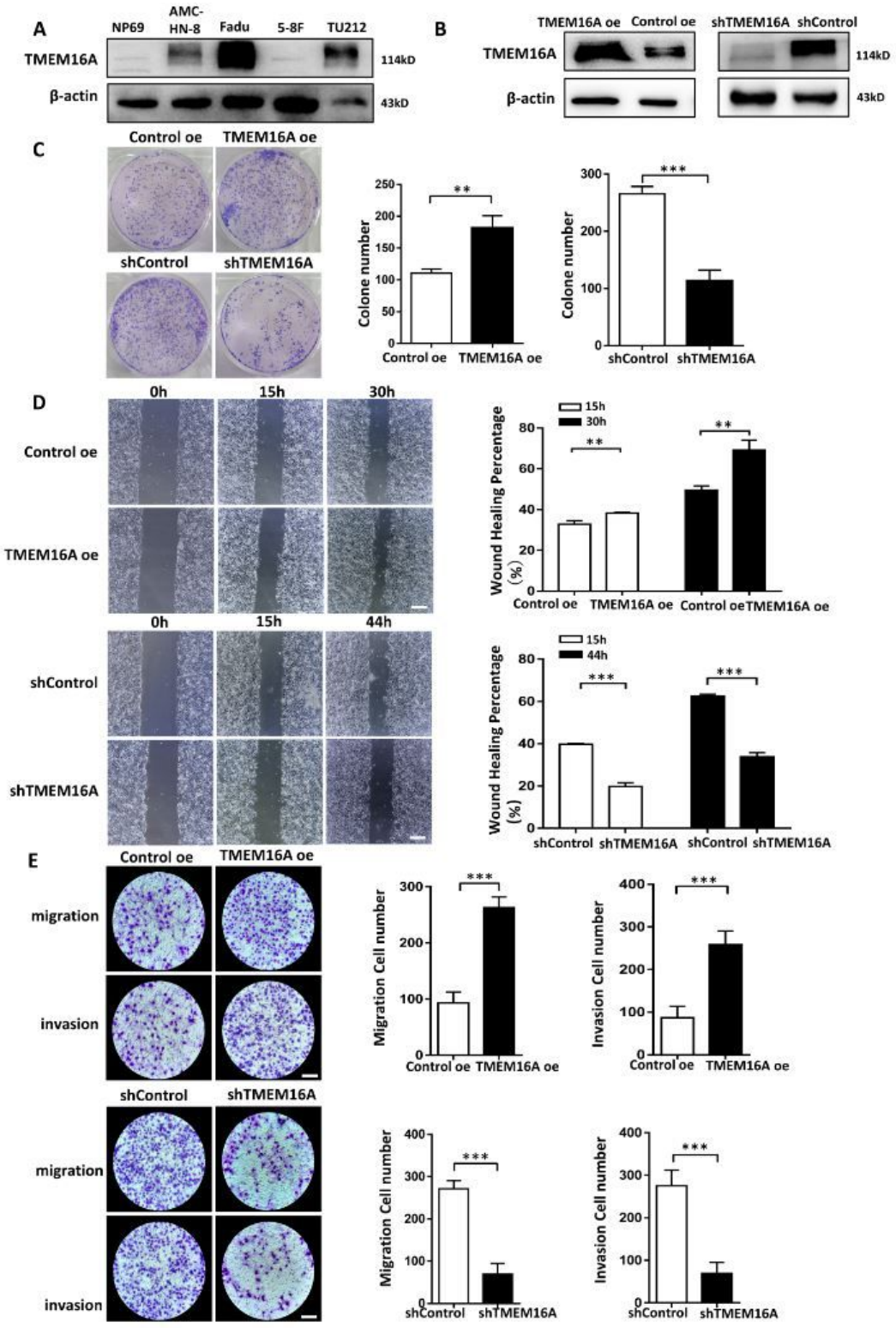

Figure 2

The effect of overexpression and down-regulation of TMEM16A on FaDu cells growth，migration and invasion *in vivo*.

A The expression of TMEM16A in HNSCC cell lines and NP69 were analyzed by western blot. **B** Western blot was used to verify that TMEM16A was effectively overexpressed or eliminated in FaDu cells. **C** After transfection of control lentivirus, shTMEM16A or overexpressed-TMEM16A, 750 cells were cultured on a six-well plate, and the overexpressed-TMEM16A group was cultured for 11 days and the shTMEM16A group was cultured for 14 days, and the average number of colonies per well was calculated. **D** Wound healing migration test: the average migration rates of FaDu cells at 0,15 and 30h treated with control lentivirus and overexpression-TMEM16A were compared. The average migration rates of FaDu cells at 0,15 and 44h treated with control lentivirus and shTMEM16A were compared. Scale bar: 100um. **E** FaDu cells were treated with control lentivirus, shTMEM16A and overexpression-TMEM16A for 48 h. After screening with puromycin, the overexpression-TMEM16A group was detected by transwell for 48 hours, and the shTMEM16A group was detected for 60 hours, and then showed the relative ratio of migratory cells to invasive cells in each visual field. All data are expressed as mean ±standard deviation. Scale: 100um; * $P < 0.05$; * * $P < 0.01$.

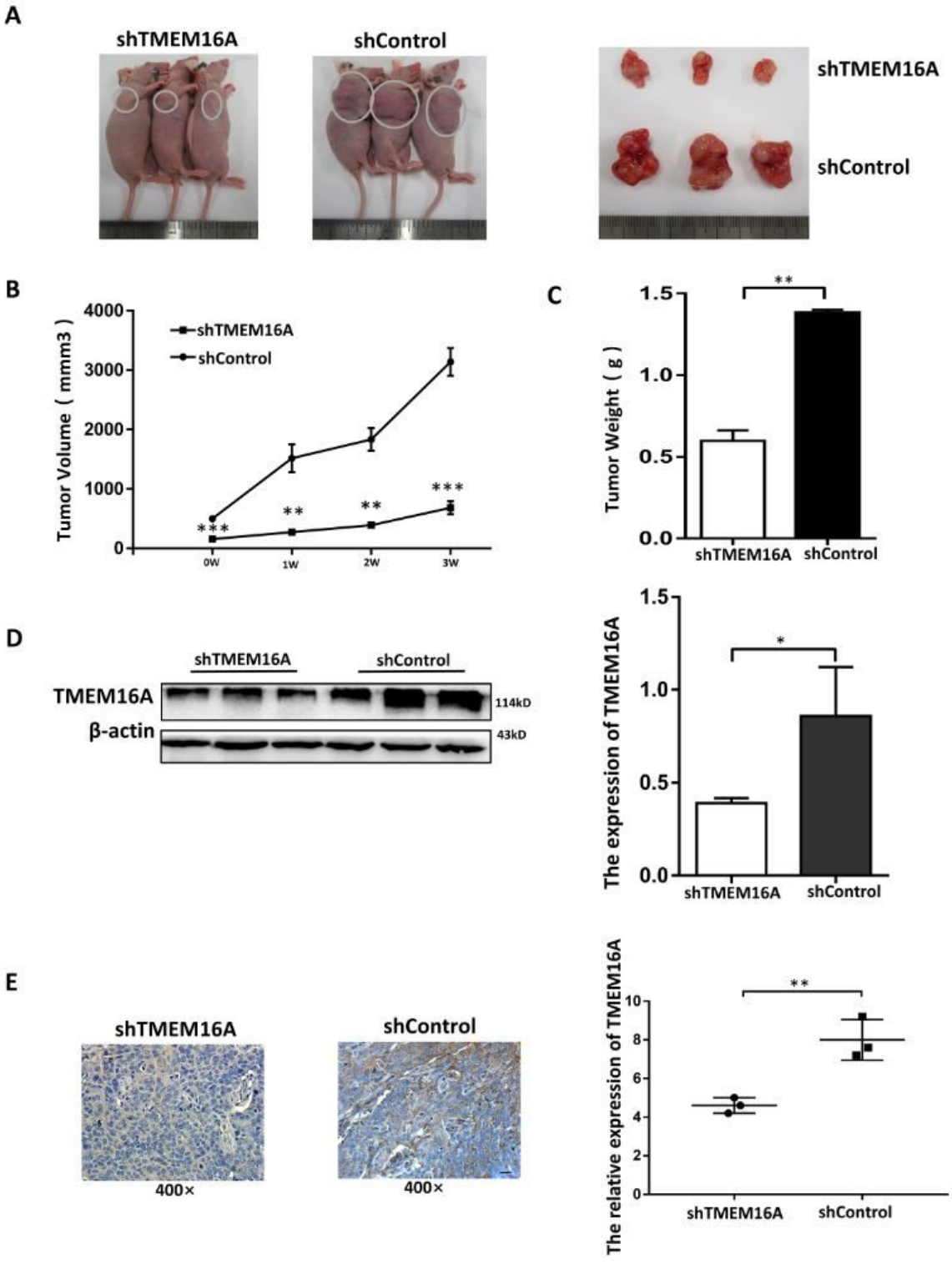

Figure 3

Down-regulation of TMEM16A suppressed tumor growth *in vivo*.

A Representative graph showing tumor growth 28 days after subcutaneously implanted FaDu cells. **B, C** Calculated tumor volume and weight in shTMEM16A and scramble groups. **D** Expression of TMEM16A as measured by western blot in shTMEM16A and scramble groups. **E** TMEM16A expression was

measured by immunohistochemistry staining in shTMEM16A and scramble groups. Scale bar: 20um; *P < 0.05, **P< 0.01.

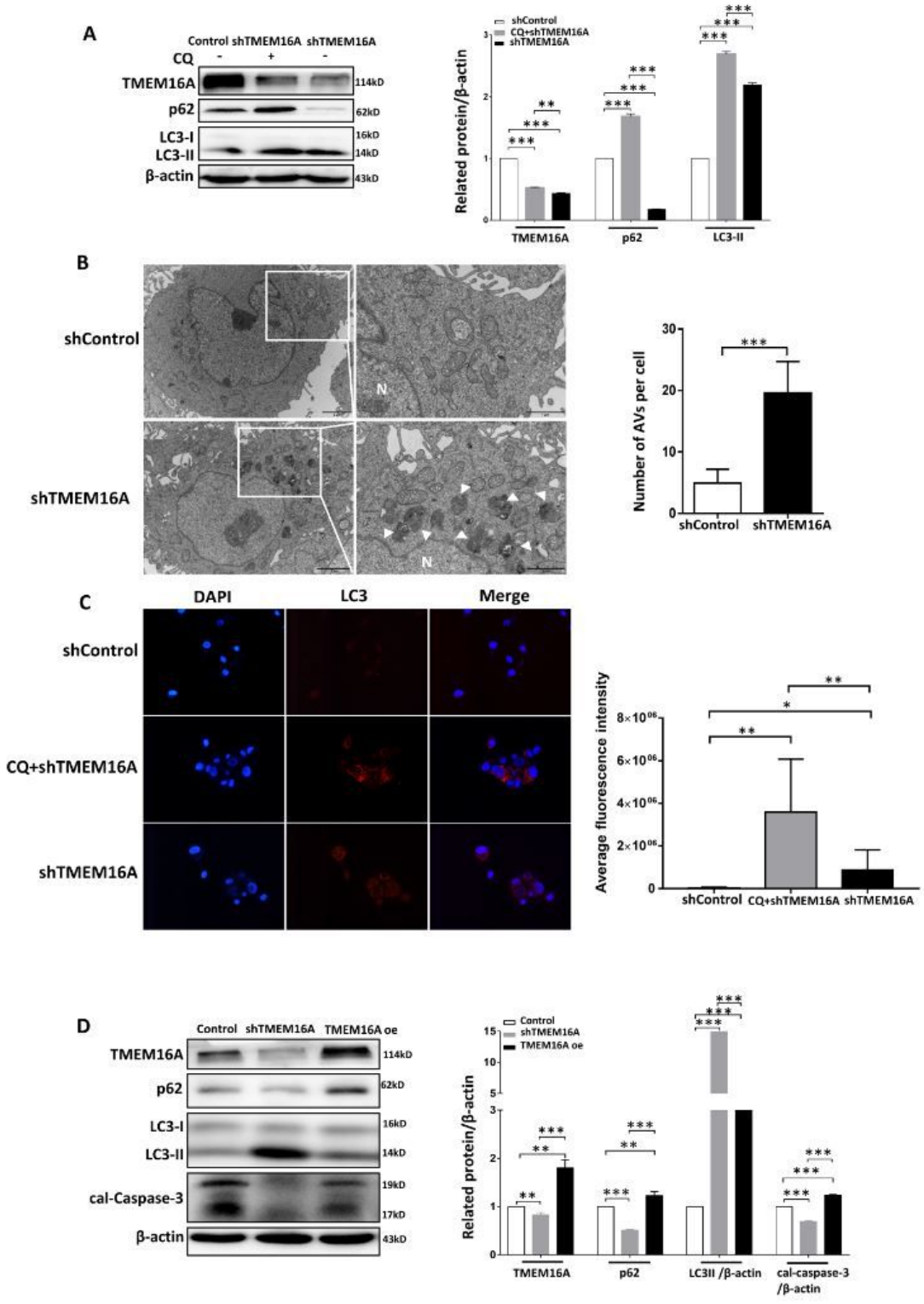

Figure 4

Down-regulation of TMEM16A induces autophagy in FaDu cells.

A FaDu cells were treated with control lentivirus or shTMEM16A for 48 hours, and then CQ (24um/mL,6h) was given to the shTMEM16A group to detect the expression of LC3-II, p62 and TMEM16A. **P < 0.01, ***P < 0.001. **B** Ultrastructural features of autophagy induced by shTMEM16A in FaDu cells. Electron micrographs were taken after the cell transfected with control and shTMEM16A. Autophagic vacuoles (AVs) were showed by white arrows. N nucleus. Scale bar: 2μm. The number of AVs was quantified from ten randomly selected cells per each group. Bars represent the mean ± standard deviation (4.90 ± 0.72 for control vs. 19.60 ± 1.61.0 for shTMEM16A). ***P <0.001. **C** Immunofluorescent staining showing the average fluorescence intensity of LC3 dot in the cell transfected with control, shTMEM16A, or CQ+shTMEM16A. Scale bar: 20μm. *P < 0.05, **P< 0.01. **D** Control lentivirus, shTMEM16A lentivirus and high expression TMEM16A lentivirus were transfected into FaDu cells for 48 hours. After screening with puromycin, the protein expressions of mTOR, cal-caspase-3, LC3-II, p62 and TMEM16A in each group were detected. **P < 0.01.

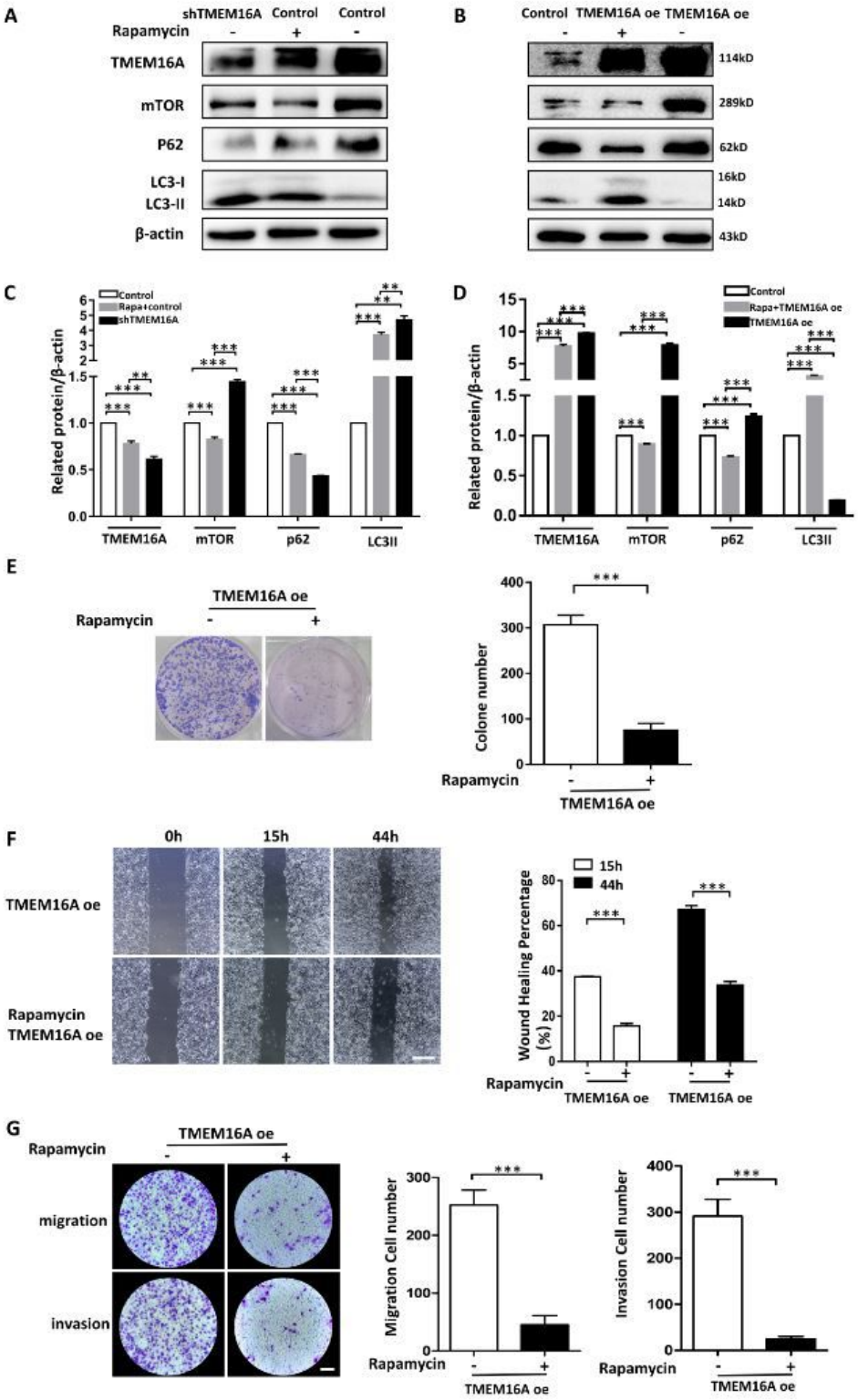

Figure 5

TMEM16A regulates autophagy through mTOR pathway and the effect of inhibition of mTOR on FaDu cells growth，migration and invasion of overexpression of TMEM16A *in vivo*.

A C In shTMEM16A group: Rapamycin (20um/mL,6h) was given to control lentivirus group, and then detect the protein expression of mTOR, LC3-II, p62 and TMEM16A in each group. **P < 0.01; ***P < 0.001.

B D In TMEM16A overexpression group: Rapamycin (20um/mL,6h) was given to overexpression TMEM16A lentivirus group, and then detect the protein expression of mTOR, LC3-II, p62 and TMEM16A in each group. **P < 0.01; ***P < 0.001.

E After transfection with overexpression-TMEM16A lentivirus, 750 FaDu cells, which added with rapamycin (20um/mL), were cultured on a six-well plate for 11 days, and the average number of colonies per well was calculated. **P < 0.01; ***P < 0.001.

F Wound healing migration test: the average migration rates of FaDu cells at 0,15 and 44h treated with overexpression-TMEM16A and overexpression-TMEM16A that added with rapamycin were compared (20um/mL). Scale bar: 500um; **P < 0.01; ***P < 0.001.

G Same as above group condition, transwell detection was performed for 48 hours to show the relative ratio of migratory cells and invasive cells in each visual field. All data are expressed as mean ±standard deviation. Scale: 100um; **P < 0.01; ***P < 0.001.

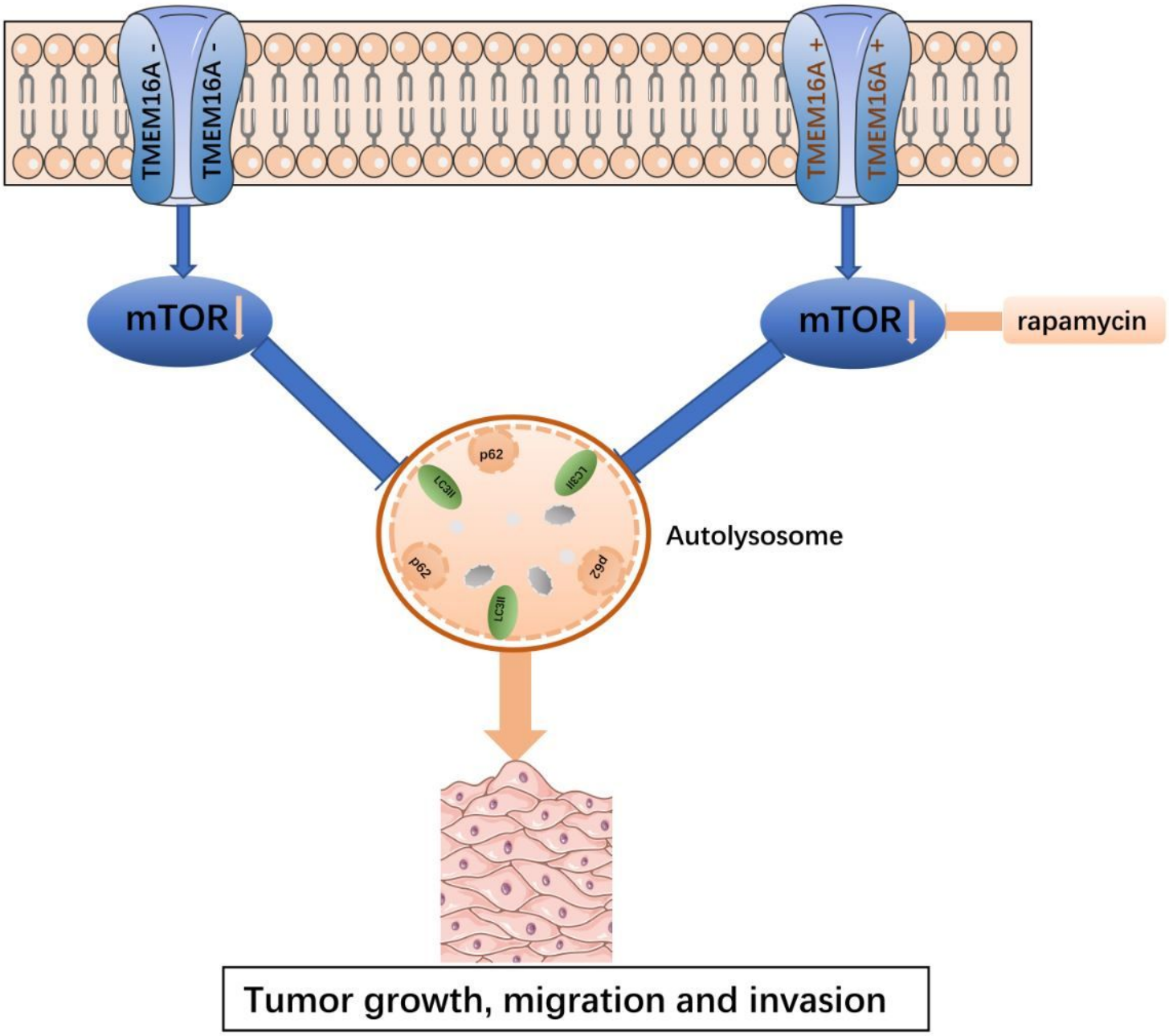

Figure 6

Schematic representation of the study findings.

Supplementary Files

This is a list of supplementary files associated with this preprint. Click to download.

- OriginalpictureofWB.pptx